SUPPLEMENTAL MATERIALS

Macrophages Promote Aortic Valve Cell Calcification and Alter STAT3 Splicing

Michael A. Raddatz[1,2], Tessa M. Huffstater[2], Matthew R. Bersi[2], Bradley I. Reinfeld[1,4], Matthew Z. Madden[1,5], Sabrina E. Booton[2], W. Kimryn Rathmell[4], Jeffrey C. Rathmell[5], Brian R. Lindman[6], Meena S. Madhur[3,7], and W. David Merryman[2]

[1]Vanderbilt University School of Medicine, [2]Department of Biomedical Engineering, and [3]Department of Molecular Physiology & Biophysics, Vanderbilt University

[4]Division of Hematology and Oncology, Department of Medicine, [5]Department of Pathology, Microbiology, and Immunology, [6]Structural Heart and Valve Center, and [7]Division of Clinical Pharmacology, Department of Medicine, Vanderbilt University Medical Center

Supplemental Methods

Bone Marrow Transplants

Two mice died 8-15 weeks into the aging period. One wild-type mouse receiving *Notch1*$^{+/-}$ bone marrow died of unknown causes, and one *Notch1*$^{+/-}$ mouse receiving *Notch1*$^{+/-}$ bone marrow died after sustaining wounds from a littermate's aggression. No other deaths occurred during the aging period.

Image Analysis

In order to determine if activated AVICs were distributed unevenly throughout the coculture landscape within any given x-y field of view, an image processing algorithm was developed to test the hypothesis that activated cells were more likely to be near macrophages. After staining, images in each channel were blurred using a Gaussian filter with a standard deviation of 4 and thresholded by Otsu's thresholding method. This mask generated positive regions, which were gated by size to identify individual cells. This process was performed in each channel to identify CD68^{+} macrophages and either RUNX2^{+} or αSMA^{+} activated AVICs.

In every image, the centroid of each activated AVIC was determined and a distance index was defined. In particular, for each identified AVIC, the location was compared to the location of each of the *n* identified macrophages and the distance to the nearest macrophage was recorded. All distances ≤ 10 μm were removed from the analysis to account for mistaken identification of one cell as both an AVIC and macrophage. Sensitivity analyses confirmed that this did not affect the conclusion. In order to determine the "expected distance" from the activated AVIC to the nearest macrophage, *N* random macrophages were placed across the x and y axes of the image and the distance from the current AVIC to the nearest random macrophage location was recorded. This randomized process was repeated 500 times in a Monte Carlo simulation, and the median distance to the nearest macrophage was recorded as the "expected distance" to the nearest macrophage. At that point, the real distance to the nearest macrophage was divided by the expected distance and recorded as the distance index of the activated AVIC. A density plot of the distance index of all activated AVICs is shown in Figure 5. The R package '*EBImage*' was used for all image processing.

Micropipette Aspiration

Capillary tubes (World Precision Instruments, Sarasota, FL) were coated with Sigmacote (MilliporeSigma, St. Louis, MO), sterilized with 70% ethanol, and allowed to dry. Coated tubes were then pulled with a P-97 micropipette puller (Sutter Instrument, Novato, CA), fractured with an MF-1 microforge (Technical Products International, St. Louis, MO) to an internal diameter of approximately 6 μm, and bent to an angle allowing for the micropipette to lie parallel to the plate upon use. Pressures were applied using a custom-built pressure regulator system with an MCFS-EZ microfluidics controller (Fluigent, Le Kremlin-Bicêtre, France).

Following treatment, AVICs were lifted with Accutase, resuspended in 500 μL MACS buffer, and kept on ice until use. Aspiration was performed on at least 10 cells from each condition and biological replicate each day. Tests were performed by linearly increasing the applied suction pressure by 8 Pa/s over 60 seconds to a final aspiration pressure of 0.48 kPa. The aspirated length of each cell was measured manually from video recorded at a rate of 2 frames/s using a microscope-mounted camera.

After all data was recorded, aspirated length of each cell was measured manually and the effective stiffness (*E*) was determined using a half-space elastic model given below:

$$E = \varphi n \left(\frac{3a}{2\pi}\right)\left(\frac{\Delta P}{L}\right)$$

where $\varphi(\eta)$ is the wall function and is equal to 2.1 (dimensionless parameter calculated from the ratio of the pipette inner radius to the wall thickness), *a* is the micropipette inner radius, and *ΔP/L* is the slope of the linear applied pressure vs. aspirated cell length curve.

Supplemental Figures

Supplemental Figure I. Confirmation of bone marrow-derived macrophage phenotype in coculture experiments.

Supplemental Figure II. Image proximity analysis workflow.

Supplemental Figure III. Raw micropipette analysis data.

Supplemental Figure IV. Wild-type and *Notch1*$^{+/-}$ bone marrow-derived macrophages.

Supplemental Figure V. Calcification quantification in wild-type and *Notch1*$^{+/-}$ mice.

Supplemental Figure VI. Echocardiography metrics in wild-type and *Notch1*$^{+/-}$ mice.

Supplemental Figure VII. MHCII^{-} macrophages in wild-type and *Notch1*$^{+/-}$ valves.

Supplemental Figure VIII. *Notch1*$^{+/-}$ macrophage migration towards AVIC-secreted media.

Supplemental Figure IX. Raw Proteome Profiler microarray results.

Supplemental Figure X. Immunofluorescence images used for image proximity analysis.

Supplemental Figure XI. RUNX2 and αSMA expression in wild-type and *Notch1*$^{+/-}$ murine valves.

Supplemental Figure XII. STAT3 splicing in AVICs exposed to macrophages.

Supplemental Figure XIII. *Adar1* transcription in cocultured AVICs.

Supplemental Figure XIV. STAT3 splicing in AVICs exposed to interferons.

Supplemental Figure XV. STAT3 splicing in human calcific aortic valve disease.

Supplemental Figure XVI. RUNX2 in human calcific aortic valve disease.

Supplemental Figure XVII. Stattic treatment of AVICs.

Supplemental Figure XVIII. STAT3 plasmid transfection.

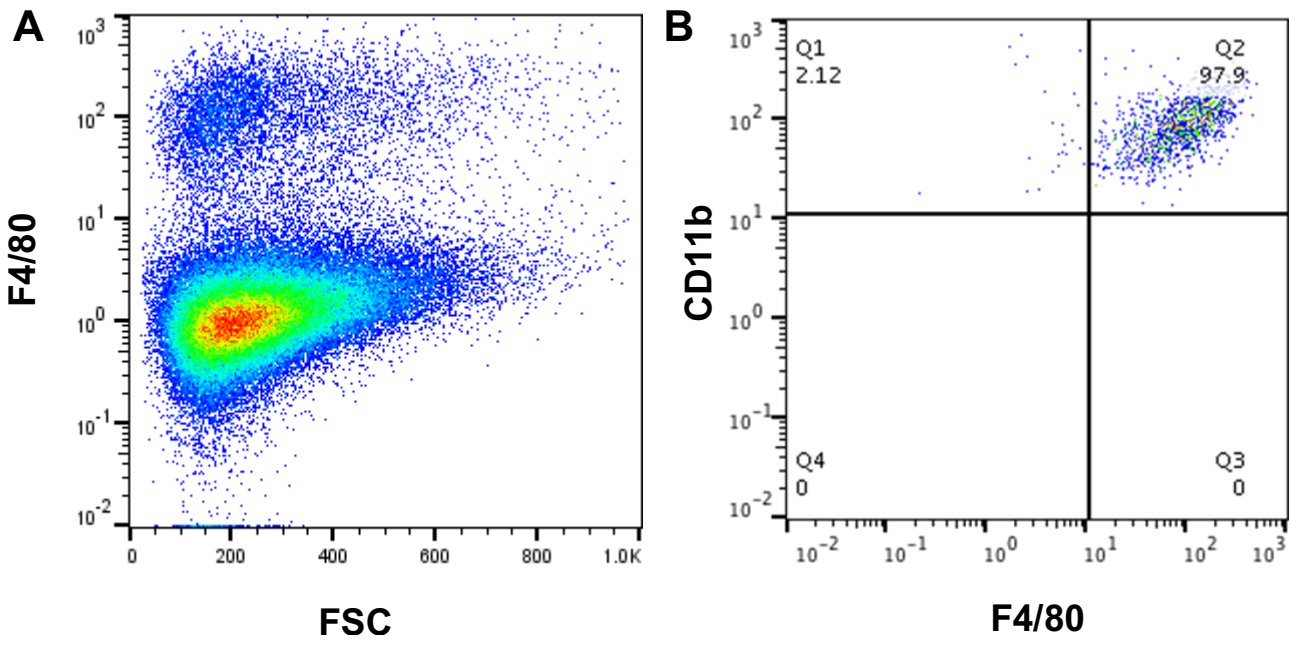

Supplemental Figure I. Confirmation of bone marrow-derived macrophage phenotype in coculture experiments. The F4/80^{hi} macrophage population is seen in AVIC-macrophage coculture (A, representative plot). Among CD45^{+} cells, >96% were CD11b^{+} and F4/80^{hi} in each of four biological replicates (B, representative plot).

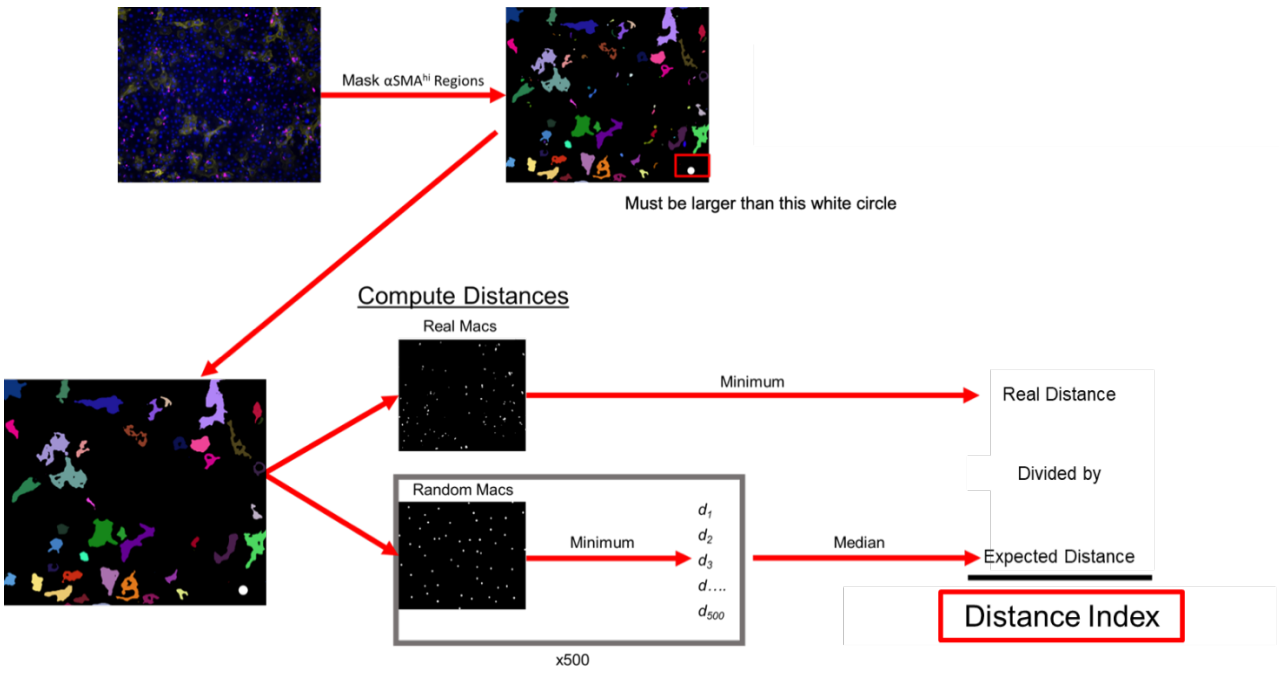

Supplemental Figure II. Image proximity analysis workflow. Images were masked for activated AVICs by RUNX2 or αSMA staining and real and expected distance to the nearest macrophage calculated. Additional details are included above in the supplemental methods.

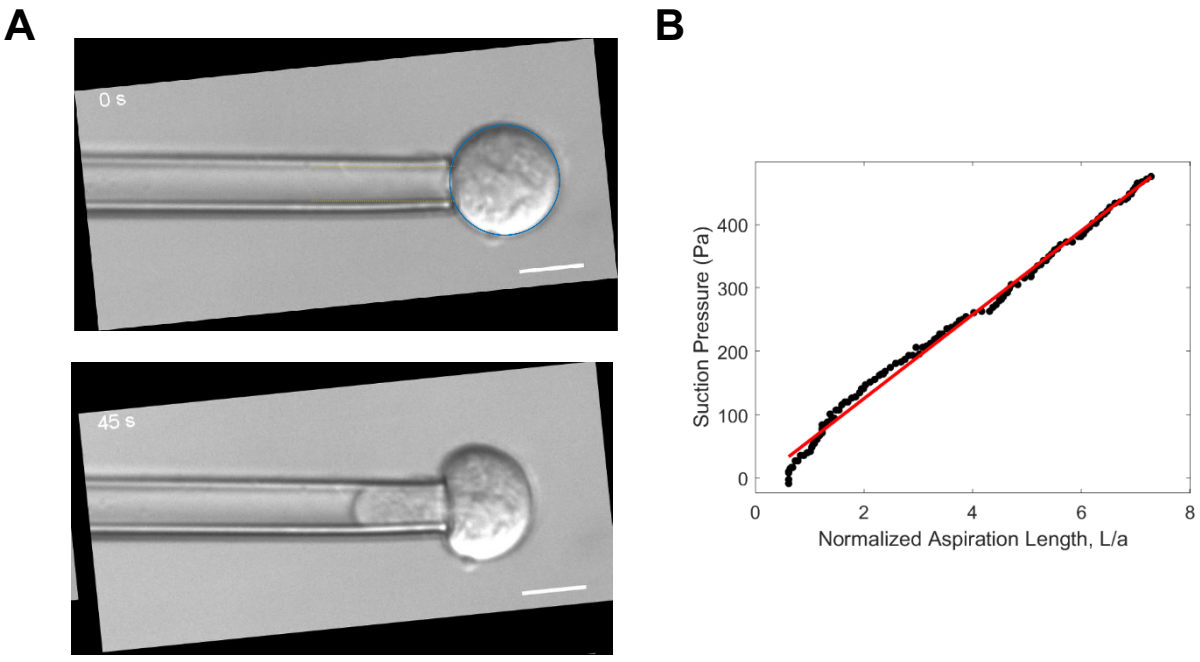

Supplemental Figure III. Raw micropipette analysis data. Stabilized images of cell aspiration were recorded (A) followed by measurement of the slope of suction pressure over normalized aspiration length to determine cellular elastic modulus (B).

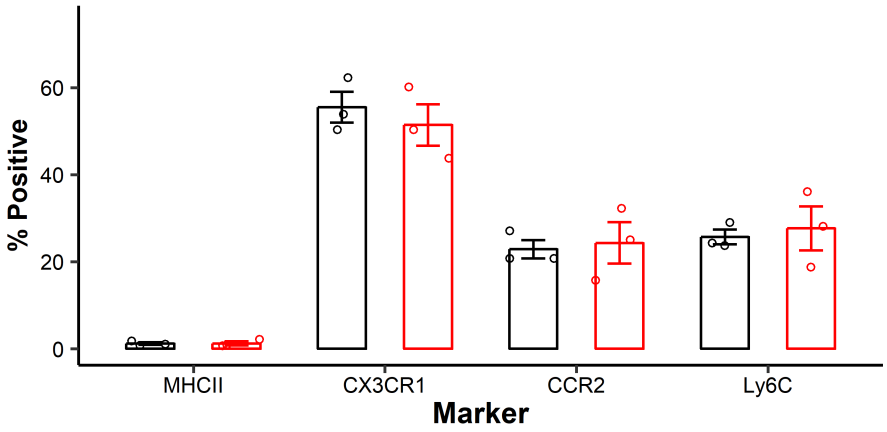

Supplemental Figure IV. Wild-type and *Notch1*$^{+/-}$ bone marrow-derived macrophages. Bone marrow-derived macrophages from wild-type (black) and *Notch1*$^{+/-}$ (red) mice have no differences in various markers of maturity. Bars represent mean ± s.e.m. All data analyzed by two-tailed *t* test.

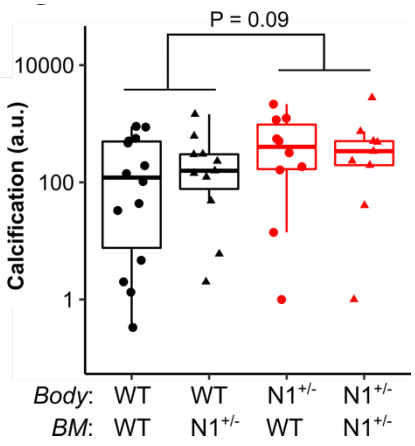

Supplemental Figure V. Calcification quantification in wild-type and *Notch1*$^{+/-}$ mice. Wild-type (WT) and *Notch1*$^{+/-}$ (N1$^{+/-}$) mice with WT and N1$^{+/-}$ bone marrow were stained for calcification with von Kossa, and positive staining was quantified. Data were analyzed by two-way aligned rank transformed ANOVA. N = 14, 11, 10, and 9 biological replicates.

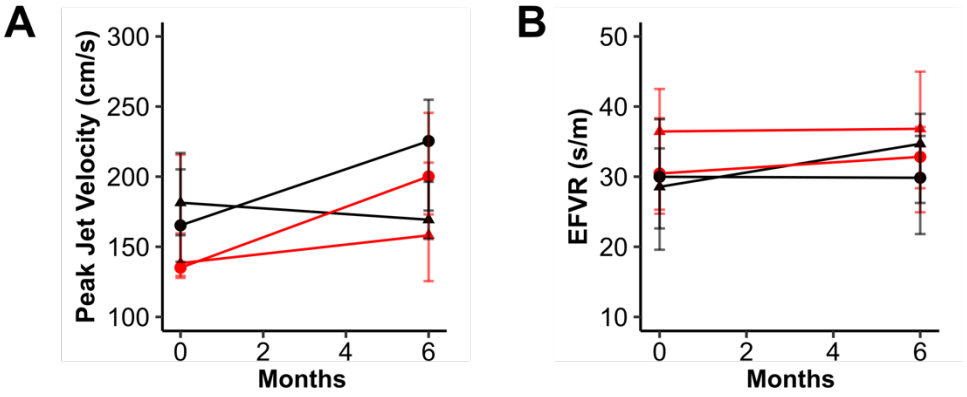

Supplemental Figure VI. Echocardiography metrics in wild-type and *Notch1*$^{+/-}$ mice. Wild-type (black) and *Notch1*$^{+/-}$ (red) mice with wild-type (circle) and *Notch1*$^{+/-}$ (triangle) bone marrow have no differences in peak jet velocity (A) or ejection fraction-velocity ratio (EFVR) (B).

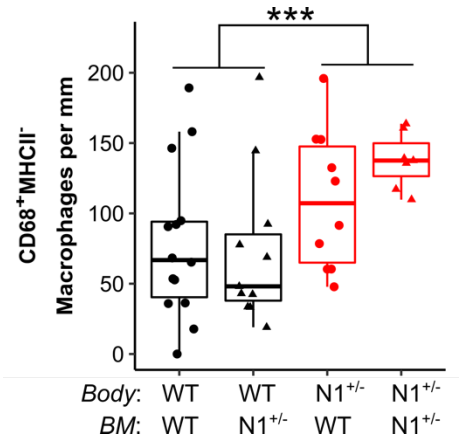

Supplemental Figure VII. MHCII$^-$ macrophages in wild-type and *Notch1*$^{+/-}$ valves. There is an increase in MHCII$^-$ macrophages in *Notch1*$^{+/-}$ mice regardless of bone marrow genotype. Boxplots display the 25th, 50th, and 75th percentiles. Data were analyzed by two-way aligned rank transformed ANOVA. ***P < 0.001. N = 14, 11, 10, and 9 biological replicates.

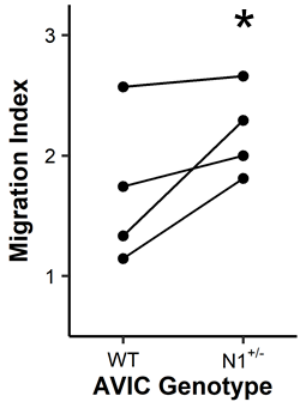

Supplemental Figure VIII. *Notch1*$^{+/-}$ macrophage migration towards AVIC-secreted media. *Notch1*$^{+/-}$ AVIC-cultured media promotes macrophage migration compared to wild-type AVIC-cultured media or uncultured media control. Data were analyzed by one-way ANOVA followed by paired, two-tailed *t* tests with Holm-Sidak corrections. *P < 0.05 from wild-type AVICs, N = biological replicates.

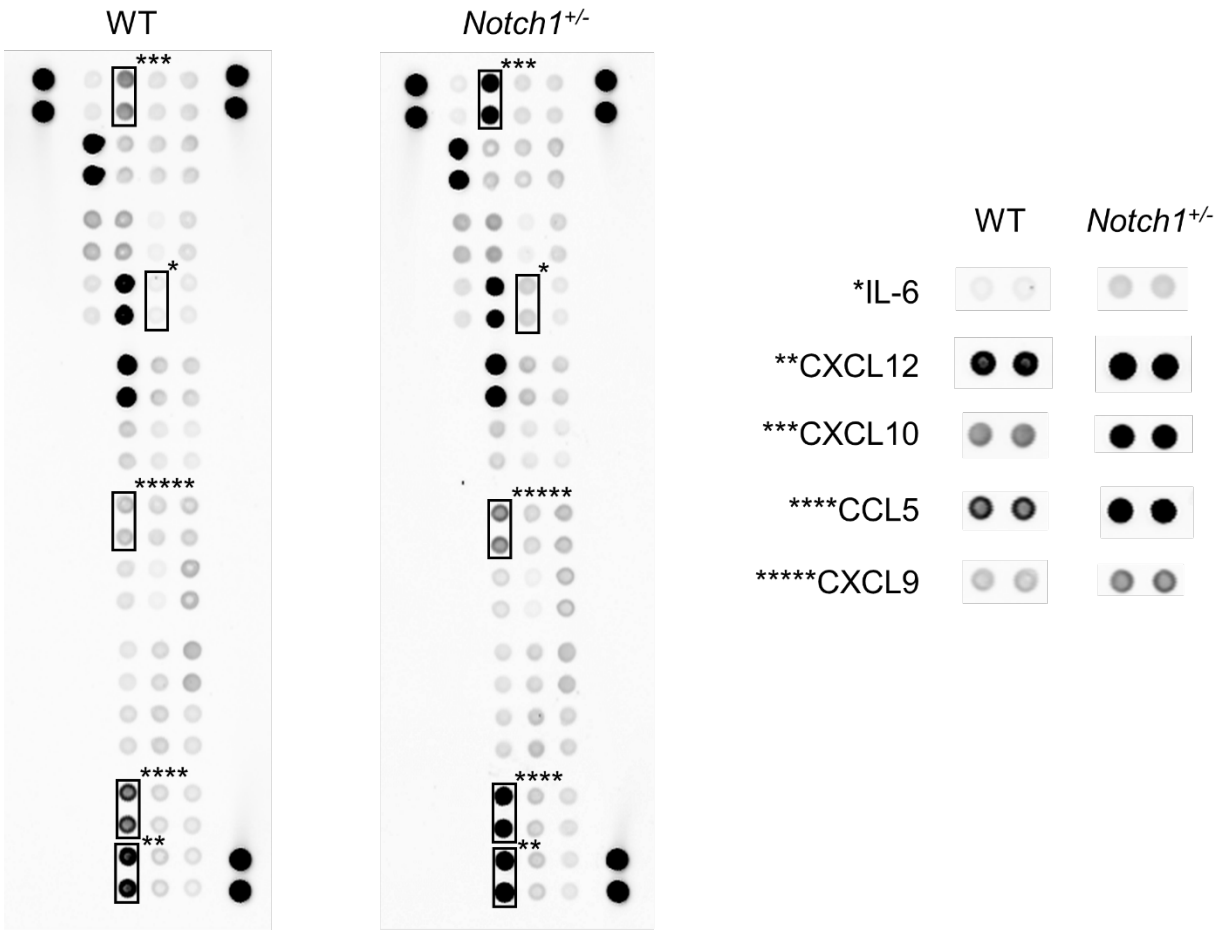

Supplemental Figure IX. Raw Proteome Profiler microarray results. Microarray of secreted factors from wild-type (WT) and *Notch1*$^{+/-}$ AVICs. *Denotes corresponding microarray spots cropped for comparison.

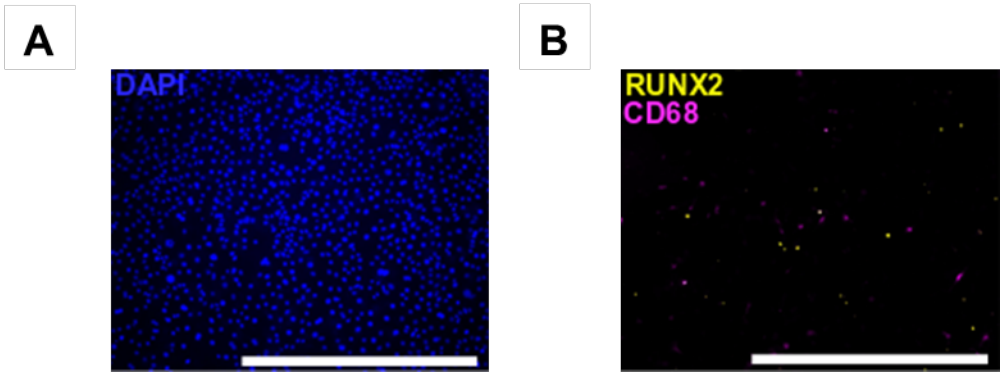

Supplemental Figure X. Immunofluorescence images used for image proximity analysis. Immunofluorescent staining of aortic valve interstitial cell and macrophage co-culture for nuclei with DAPI (blue) (A) and for identification of osteogenic calcification of aortic valve interstitial cells (RUNX2, yellow) and macrophage (CD68, pink) (B).

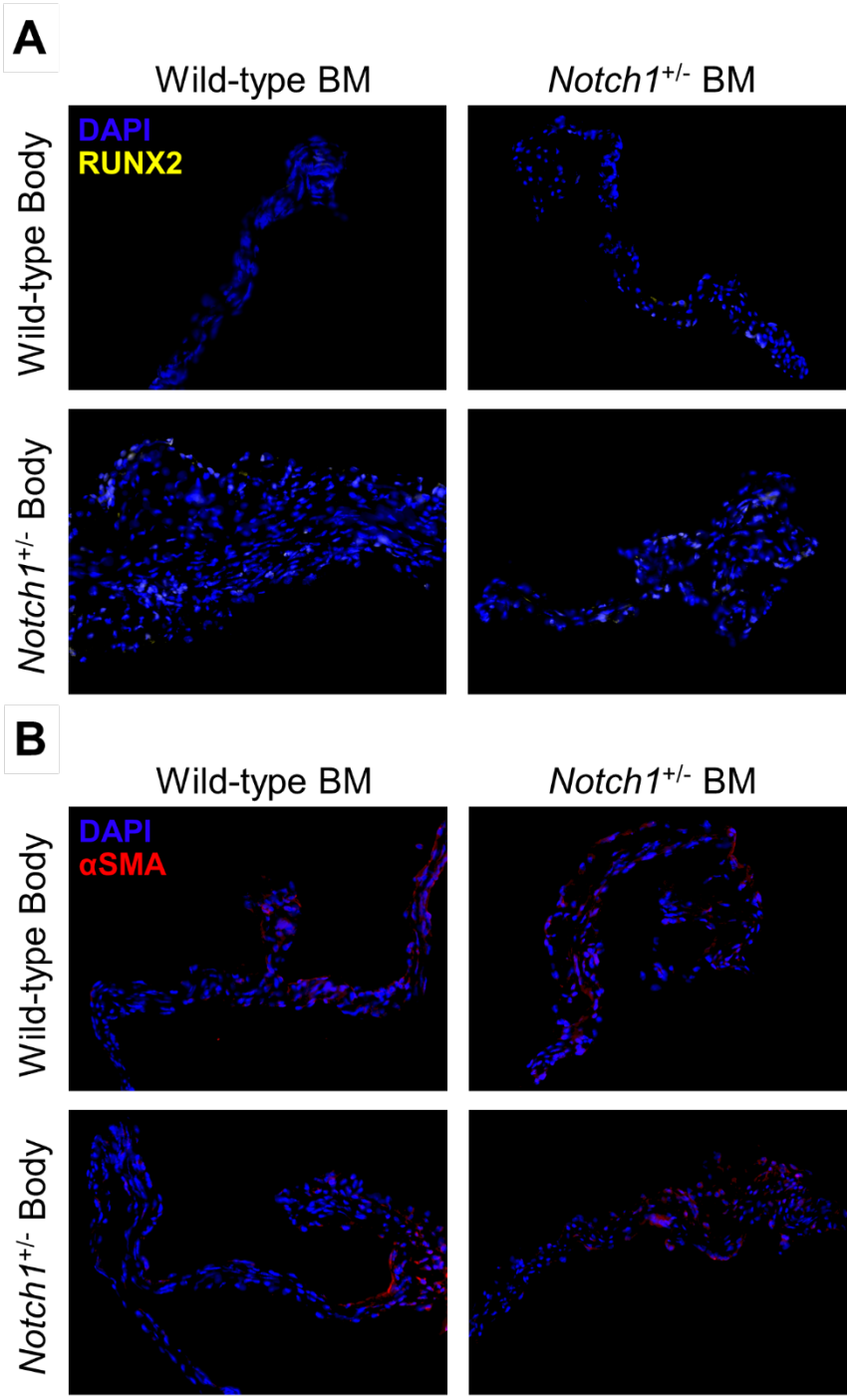

Supplemental Figure XI. RUNX2 and αSMA expression in wild-type and *Notch1*$^{+/-}$ murine valves. Immunofluorescence staining of RUNX2 (A, yellow, white when overlapped with DAPI) and αSMA (B, red) in valves from wild-type (WT) and *Notch1*$^{+/-}$ (N1$^{+/-}$) mice transplanted with WT or N1$^{+/-}$ bone marrow (BM).

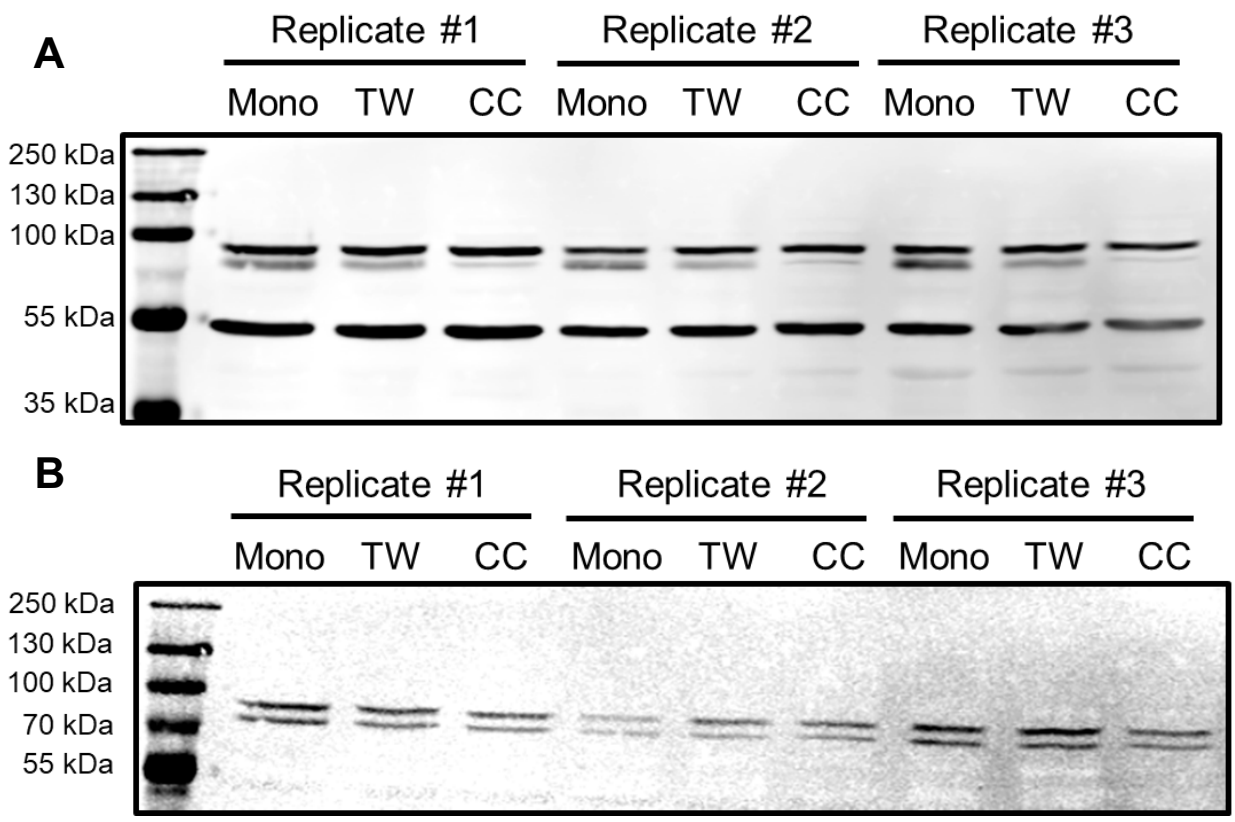

Supplemental Figure XII. STAT3 splicing in AVICs exposed to macrophages. Raw Western blot data for STAT3 splicing (A) and phosphorylation (B) in AVICs in monoculture (Mono), Transwell culture (TW), or direct coculture (CC) with macrophages. p/STAT3α is stained at ~88 kDa with p/STAT3β just below. Loading control is α-Tubulin stained at ~50 kDa (A). STAT3 is visualized with anti-mouse IgG2a secondary antibody in the 700 channel, pSTAT3 with anti-rabbit IgG secondary antibody in the 800 channel, and α-Tubulin with anti-mouse IgG1 secondary antibody in the 700 channel.

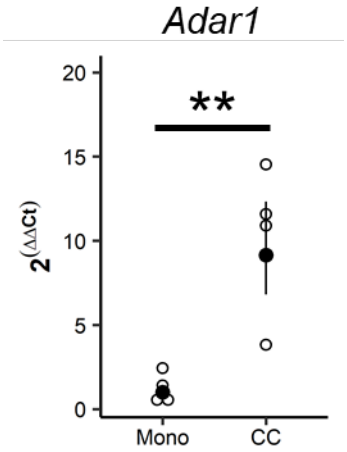

Supplemental Figure XIII. *Adar1* transcription in cocultured AVICs. Coculture of AVICs with macrophages increases transcription of *Adar1*. Summary data represent the mean ± s.e.m. **P < 0.01 by two-tailed *t* test.

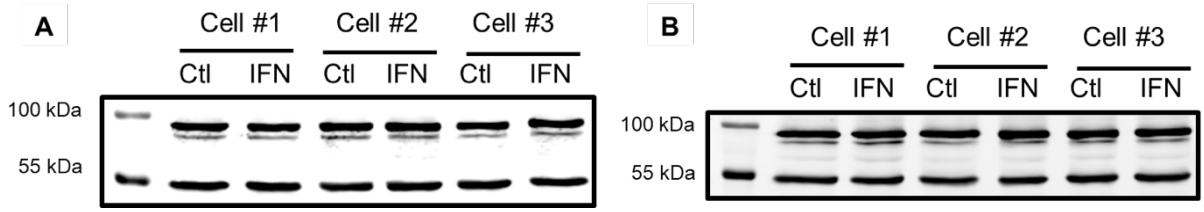

Supplemental Figure XIV. STAT3 splicing in AVICs exposed to interferons. Culture of AVICs with either interferon (IFN) -alpha (A) or -gamma (B) does not affect STAT3 splicing. STAT3α is stained at ~88 kDa with STAT3β just below. Loading control is α-Tubulin stained at ~50 kDa.

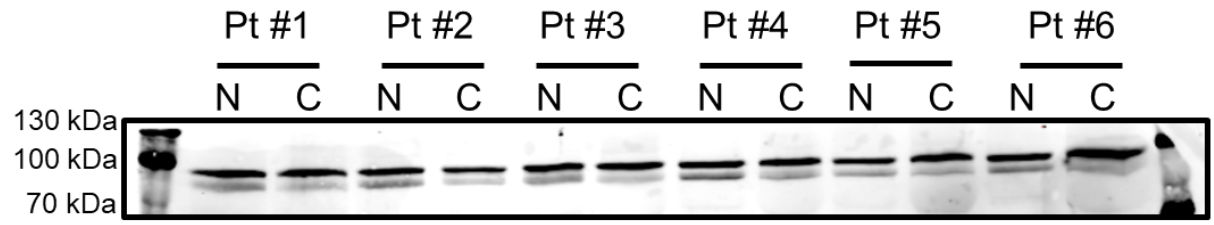

Supplemental Figure XV. STAT3 splicing in human calcific aortic valve disease. Representative raw Western blot data for STAT3 splicing in non-calcified (N) and calcified (C) tissue from patients with calcific aortic valve disease. STAT3α is stained at ~88 kDa with STAT3β just below. Total STAT3 quantified from previous Western blot was used as loading control in order to normalize STAT3β to total STAT3. STAT3 is visualized with anti-mouse IgG2a secondary antibody in the 700 channel.

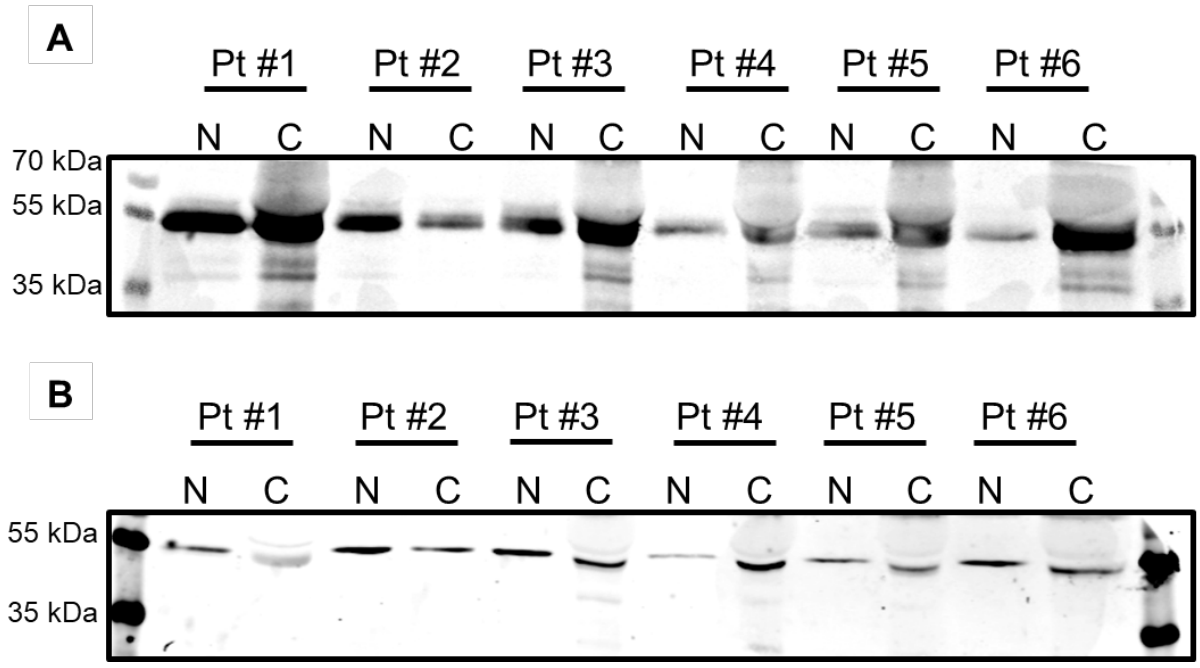

Supplemental Figure XVI. RUNX2 in human calcific aortic valve disease. Representative raw Western blot data for RUNX2 expression in non-calcified (N) and calcified (C) tissue from patients with calcific aortic valve disease. RUNX2 is stained at ~56 kDa (A). Loading control is α-Tubulin stained at ~50 kDa (B). RUNX2 is visualized with anti-rabbit IgG1 secondary antibody in the 800 channel and α-Tubulin is visualized with anti-mouse IgG1 secondary antibody in the 700 channel. Although they are in separate channels, RUNX2 was stained first followed by α-Tubulin to prevent any bleedover of α-Tubulin signal into RUNX2 densitometry quantification.

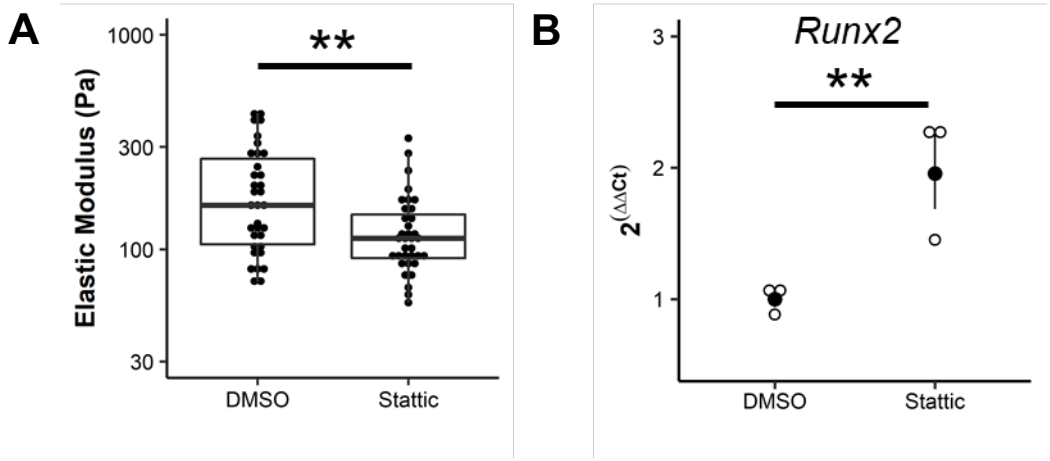

Supplemental Figure XVII. Stattic treatment of AVICs. Treatment with 10 μM Stattic for two hours decreases cellular stiffness (A) but increases *Runx2* transcription measured after 10 additional hours in complete DMEM media (B). Boxplots display the 25th, 50th, and 75th percentiles. Summary data represent the mean ± s.e.m. (B). **P < 0.01 by Mann Whitney *U* test (A) or two-tailed *t* test on untransformed ΔCt values (B).

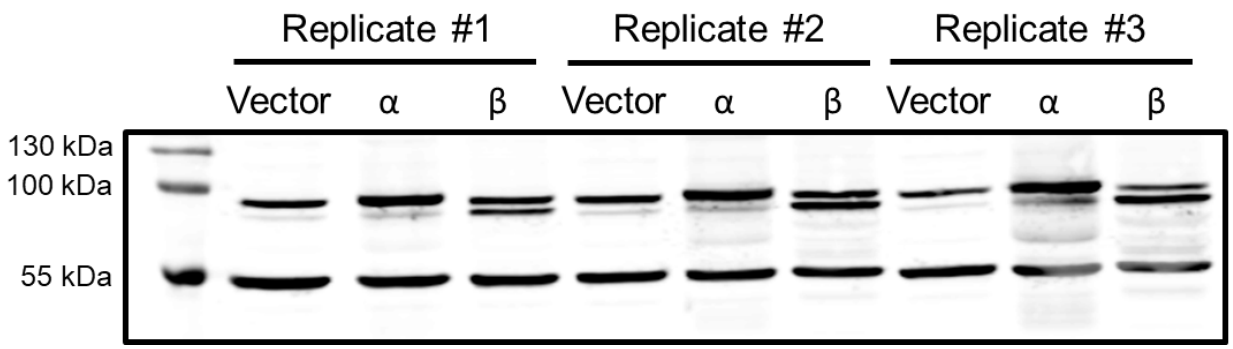

Supplemental Figure XVIII. STAT3 plasmid transfection. Representative raw Western blot data for STAT3 expression in samples transfected with empty vector plasmid (Vector), STAT3α overexpression plasmid (α), or STAT3β overexpression plasmid (β). STAT3α is stained at ~88 kDa with STAT3β just below. Loading control is α-Tubulin stained at ~50 kDa. STAT3 is visualized with anti-mouse IgG2a secondary antibody and α-Tubulin is visualized with anti-mouse IgG1 secondary antibody: both in the 700 channel.

Major Resources Tables

Animals (in vivo studies)

Species	Vendor or Source	Background Strain	Sex
Mus musculus	The Jackson Laboratory	C57BL/6J; *Notch1*$^{+/-}$	80 x M (BMT, BMM, FC, IF) 45 x F (BMT, BMM)

Animal breeding

	Species	Vendor or Source	Background Strain	Other Information
Parent	*Mus musculus*	The Jackson Laboratory, Bar Harbor, ME	C57BL/6J	Breedings were between *Notch1*$^{+/-}$ and *Notch1*$^{+/+}$ animals backcrossed onto a C57BL/6J background to produce wild-type and *Notch1*$^{+/-}$ littermate controls
Parent	*Mus musculus*	Merryman Lab from Rossant Lab, University of Toronto	C57BL/6J; *Notch1*$^{+/-}$	Breedings were between *Notch1*$^{+/-}$ and *Notch1*$^{+/+}$ animals on a C57BL/6J background to produce wild-type and *Notch1*$^{+/-}$ littermate controls

Antibodies

Target antigen	Vendor or Source	Catalog #	Working concentration	Lot # (preferred but not required)
αSMA-Cy5.5	MilliporeSigma	C6198	IF(1:300)	058M4761V
α-Tubulin	Vanderbilt Molecular Biology Core	n/a	WB(1:1000)	n/a
CCR2-PE	BioLegend	150609	FC(1:50)	B278733
CD11b-e450	Thermo Fisher	48-0112-82	FC(1:400)	4329941
CD45-BV510	BD Biosciences	563891	FC(1:800)	9066967
CD68-AF594	BioLegend	137020	IF(1:200)	B239125
CX3CR1-PerCP/Cy5.5	BioLegend	149009	FC(1:250)	B271940
F4/80-PE/Cy7	BioLegend	123114	FC(1:400)	B265636
IL-6	Abcam	ab6672	IF(1:200)	GR3195128-21
Ly6C-FITC	BioLegend	128006	FC(1:700)	B270133
MHCII-APC	BioLegend	107614	FC(1:1600)	B255462
MHCII-FITC	Thermo Fisher	11-5321-82	IF(1:100)	4322171
Rabbit IgG-AF 647	Invitrogen	A21245	IF(1:300)	1837984
Rabbit IgG-FITC	Abcam	ab6717	IF(1:300)	731506
RUNX2	Novus Biologicals	NBP1-77461	IF(1:100)	B-1
RUNX2	Cell Signaling	12556S	WB(1:1000)	2
STAT3	Cell Signaling	9139S	WB(1:1000)	12
pSTAT3 (Y705)	Cell Signaling	9145S	WB(1:2000)	34

Cultured Cells

Name	Vendor or Source	Sex (F, M, or unknown)
Immortalized wild-type AVICs	Immorto Mice	2 x M, 3 x F
Immortalized *Notch1*$^{+/-}$ AVICs	Immorto Mice	2 x M, 2 x F
Bone marrow-derived macrophages	Wild-type and *Notch1*$^{+/-}$ mice	12 x M, 12 x F

Primers for qRT-PCR

Target Transcript	Forward Primer (5' to 3')	Reverse Primer (5' to 3')
Acta2	TCTGGACGTACAACTGGTATTG	GGCAGTAGTCACGAAGGAATAG
Adar1	CGGCACTATGTCTCAAGGGT	TGCGGGTATCTCCACTTGCT
Cdh11	ACACCATGAGAAGGGCAAG	ACCGGAGTCAATGTCAGAATG
Gapdh	ATGACAATGAATACGGCTACAG	TCTCTTGCTCAGTGTCCTTG
Icam1	GCAGAGGACCTTAACAGTCTAC	TGGGCTTCACACTTCACAG
Il6	CAAAGCCAGAGTCCTTCAGAG	GAGCATTGGAAATTGGGGTAG
Runx2	CCCAGCCACCTTTACCTACA	TATGGAGTGCTGCTGGTCTG
Sparc	CTGTCCCGGGTGATGGTATG	TGGAGTGTTTGCTTCTGTGC
Spp1	GTGATTTGCTTTTGCCTGTTTG	GAGATTCTGCTTCTGAGATGGG
Vegfa	AGTCTGTGCTCTGGGATTTG	GTTGGCACGATTTAAGAGGGG